A Spin-phony in Monte Carlo: Simulating the 2D Ising Model

Gabriel Matos[1]

[1] *Department of Physics, Columbia University, New York, NY 10027*

We present a simulation of the 2D Ising model using the Metropolis algorithm for lattice sizes $L = 10$, 16, 24, and 36. The distributions of energy E, magnetization M, heat capacity C, and magnetic susceptibility χ as a function of temperature are shown, and finite-size scaling effects are discussed. We provide a numerical estimation of the critical temperature T_c associated with the magnetic phase transition of the system.

I. INTRODUCTION

The Ising model is a simplified model of a(n) (anti-)ferromagnet undergoing a magnetic phase transition in dimensions $d > 1$. It is described by a lattice of spin-1/2 particles where each spin lives in a site in the lattice. The spins are able to interact with their nearest neighbors with an interaction strength constant J, and with an external magnetic field B, giving a Hamiltonian

$$H = -J \sum_{\langle i,j \rangle} S_i S_j - \mu B \sum_{i=1}^{N} S_i. \tag{1}$$

Here $\sum_{\langle i,j \rangle}$ describes the sum between nearest neighbors, and we consider a total number of N spins. In this paper, we will be simulating a 2-dimensional (2D) Ising model using the Metropolis algorithm on a lattice of dimensions $L \times L$, such that the total number of spins is $N = L \times L$. We will use finite-size scaling to extrapolate these results to the $L \to \infty$ limit. The structure of the subsequent sections is as follows: Sec. II will give some theoretical background, including a description of the Metropolis algorithm; Sec. III will outline the simulation setup and results; and Sec. IV will present concluding remarks. The entire set of Python scripts utilized in this analysis can be found on github [1]. The following discussion follows closely the outline of problem 7.9.1 in [2], as described in the Appendix.

II. THEORETICAL BACKGROUND

Markov Processes, Detailed Balance, and Convergence

In statistical physics, the probability that a configuration of a system occurs is given by the Boltzmann weight of the given configuration,

$$P_\nu = \frac{1}{Z} e^{-\beta E_\nu}. \tag{2}$$

Here Z is the partition function,

$$Z = \mathrm{Tr} e^{-\beta \hat{H}}. \tag{3}$$

We can compute the expectation values of quantities of interest by then averaging according to this probability distribution, namely

$$.\langle A \rangle = \frac{1}{Z} \mathrm{Tr} A e^{-\beta \hat{H}} = \frac{1}{Z} \sum_{\nu} A(\nu) e^{-\beta E_\nu}. \tag{4}$$

In turn, one way of simulating the system numerically is by generating many configurations according to the probability distribution P_ν, calculating the observable A for each, and then computing a simple average. To accomplish this, note that the rate of change of the probability of finding a configuration ν of the system as a function of time is given by

$$\frac{\mathrm{d}P_\nu(t)}{\mathrm{d}t} = \sum_{\sigma} \left(P_\sigma(t) W(\sigma \to \nu) - P_\nu(t) W(\nu \to \sigma) \right), \tag{5}$$

where $P_\nu(t)$ is the probability of having configuration ν at time t, while $W(\sigma \to \nu)$ is the probability per unit time of going from configuration σ to ν. It follows logically that

$$\sum_{\sigma} W(\nu \to \sigma) = 1, \quad \sum_{\nu} P_\nu(t) = 1, \tag{6}$$

since the probability of going from ν to any other configuration must be 1, and the probability of finding the system in some configuration ν must also be 1. If we then enforce that in the long-time limit the probability distribution P_ν approaches the Boltzmann distribution, and that going from any one configuration to the next is both a Markov process and ergodic, we find from equation 5 (in the stationary limit where $\mathrm{d}P_\nu/\mathrm{d}t = 0$),

$$\sum_{\sigma} P_\sigma W(\sigma \to \nu) = \sum_{\sigma} P_\nu W(\nu \to \sigma). \tag{7}$$

We further impose the condition of detailed balance

$$P_\sigma W(\sigma \to \nu) = P_\nu W(\nu \to \sigma), \tag{8}$$

from which in the long-time limit, setting P_ν to be the Boltzmann distribution, implies both

$$\frac{P_\sigma}{P_\nu} = e^{-\beta(E_\sigma - E_\nu)}, \tag{9}$$

$$\frac{W(\nu \to \sigma)}{W(\sigma \to \nu)} = \frac{P_\sigma}{P_\nu} = e^{-\beta(E_\sigma - E_\nu)}. \tag{10}$$

It follows that if we choose $W(\nu \to \sigma)$ to satisfy equation 10, in the long-time limit the the probability distribution will approach the Boltzmann distribution.

The Metropolis Algorithm

There are many possible choices for $W(\nu \to \sigma)$, where the one to be utilized in this paper is that of Metropolis,

$$\begin{cases} W(\nu \to \sigma) = 1 & \text{for } P_\sigma \geq P_\nu \ (E_\sigma \leq E_\nu) \\ W(\nu \to \sigma) = \frac{P_\sigma}{P_\nu} & \text{for } P_\sigma < P_\nu \ (E_\sigma > E_\nu). \end{cases} \tag{11}$$

This option satisfies detailed balance. For instance if we started in configuration ν where $P_\sigma > P_\nu$, then $W(\nu \to \sigma) = 1$ and $W(\sigma \to \nu) = P_\nu / P_\sigma$. It follows

$$P_\sigma W(\sigma \to \nu) = P_\sigma P_\nu / P_\sigma = P_\nu \times 1 = P_\nu W(\nu \to \sigma).$$

Similarly, if $P_\sigma < P_\nu$, then $W(\nu \to \sigma) = P_\sigma / P_\nu$ and $W(\sigma \to \nu) = 1$. Therefore,

$$P_\sigma W(\sigma \to \nu) = P_\sigma \times 1 = P_\sigma \frac{P_\nu}{P_\sigma} = P_\nu W(\nu \to \sigma)$$

In turn, simulating a system to generate configurations according to the Boltzmann probability distribution requires us to implement a numerical algorithm that at each time step, makes a decision of whether to transition from a state $\nu \to \sigma$ according to the Metropolis prescription above. If we let this algorithm run for a long time (a thermalization period), we will then generate configurations according to the desired P_ν. This is the approach we will take to simulate the 2D Ising model in the following section.

III. SIMULATION

Simulation Setup and Parameters

We will be simulating the 2D Ising model in the case of no magnetic field. The Hamiltonian then only has the nearest neighbor interaction,

$$H = -J \sum_{\langle i,j \rangle} S_i S_j. \tag{12}$$

We will take periodic boundary conditions and simulate the system for various system lengths L, where $N = L \times L$. In particular, we will be simulating for L =10, 16, 24, and 36, and 300 temperature points, where T will range from 0.015 to 4.5 in steps of 0.015. Here temperature will be measured in units of J, where we set $k_B = 1$. We will be following the Metropolis algorithm as follows:

1. An arbitrary configuration of Ising spins will first be selected (because of ergodicity, the system will equilibrate regardless of the initial condition).
2. We will then choose a site at random and flip its spin. The Boltzmann weights of the pre-flip configuration is P_{old} and post-flip P_{new}.
3. We will then generate a random number r uniformly between 0 and 1
4. If $P_{\text{new}}/P_{\text{old}} \geq r$, we accept the change. Otherwise reject it.
5. We then repeat steps 2-4 for a total of $N = L \times L$ times. This will count as a "sweep".

From our starting configuration, we will be performing 10^5 sweeps to allow the system to thermalize. Then, we will be performing 3×10^5 sweeps, performing measurements at every 10 sweeps to get good statistics. This will be repeated for each one of the 300 temperature points, for each lattice size. For low temperatures, the system is more likely to thermalize if we start with all spins aligned either up or down. We will be following this prescription for $T < 1$. The entire simulation time for all lattice sizes is on the order of 30 minutes.

We will be measuring the following quantities in this simulation: the energy E/N per spin of the system,

$$\frac{E}{N} = \frac{\langle H \rangle}{N}; \tag{13}$$

the specific heat C,

$$C = \frac{1}{N k_b T^2} \left(\langle H^2 \rangle \langle H \rangle^2 \right); \tag{14}$$

the magnetization per site M,

$$M = \langle S_i \rangle; \tag{15}$$

and the magnetic susceptibility χ,

$$\chi = \frac{N}{k_b T} \left(\langle \frac{1}{N} | \sum S_i |^2 \rangle - \langle S_i \rangle^2 \right). \tag{16}$$

Results

The energy per spin as a function of T is shown in Fig. 1. We observe that the energy per spin is lowest at low temperatures, as in this regime all spins are aligned. As the temperature rises, the spin orientation becomes randomized, and we see a monotonic increase in the energy per spin. For all lattice sizes, there's a sharp rise in E/N between temperatures $2 \leq T \leq 3$. This produces an inflection point from which the spins prefer to be aligned to randomized. We will see the inflection point happens at around the critical temperature T_c, associated with a phase transition of the system.

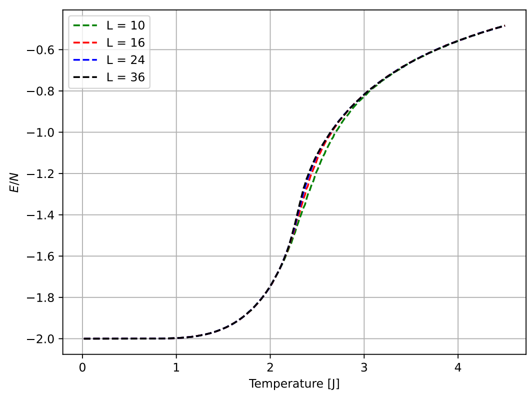

FIG. 1: The energy per spin as a function of temperature.

The susceptibility as a function of T is shown in Fig. 2, where both the temperature where the peak in χ is located, T_c and the value at the peak, χ_c are shown.

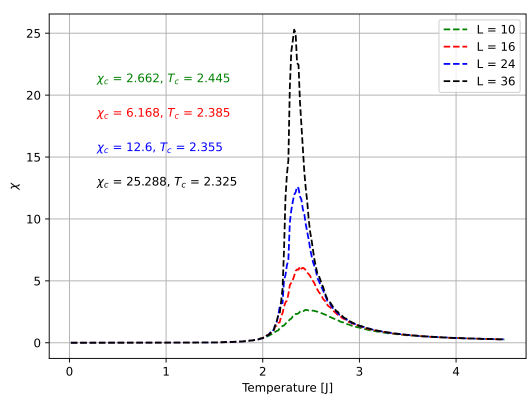

FIG. 2: The susceptibility as a function of temperature.

Fig. 3 shows the peak temperature T_c plotted as a function of L^{-1}. We utilize this and the following finite-size scaling relation

$$T_c(L) = T_c + (x_0 T_c) L^{-\nu}, \tag{17}$$

where we assume $\nu = 1$, to determine the real T_c as $L \to \infty$ through a linear fit. We find that $T_c = 2.283$. This deviates from the exact value of $\hat{T}_c = 2.269185$ by 0.61%.

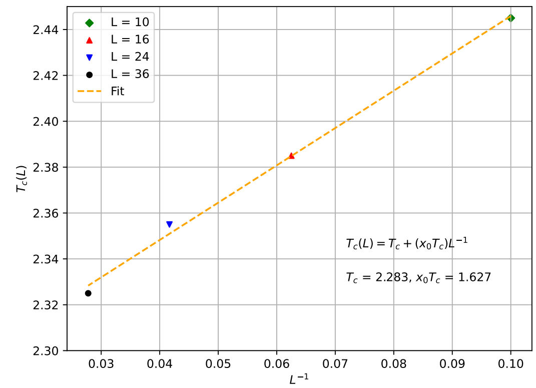

FIG. 3: $T_c(L)$ as a function of L^{-1}, with a linear fit of Eqn. 17

.

Plotting the maximum susceptibility as a function of L should yield a power-law

$$\chi \propto L^{\gamma/\nu}. \tag{18}$$

We determine the value of the exponent γ/ν by performing a linear fit of $\ln(\chi_c)$ versus $\ln(L)$, which is shown in Fig. 4. This yields a value of $\gamma/\nu = 1.758$, which deviates from the accepted value of 1.75 by 0.46%. Fig. 5 shows $L^{-\gamma/\nu}\chi$ plotted as function of the scaling variable $L^{1/\nu}(T - T_c(L))$ (where here ν is taken to be 1 again). We observe that the curves for all system sizes collapse onto each other near the critical temperature T_c.

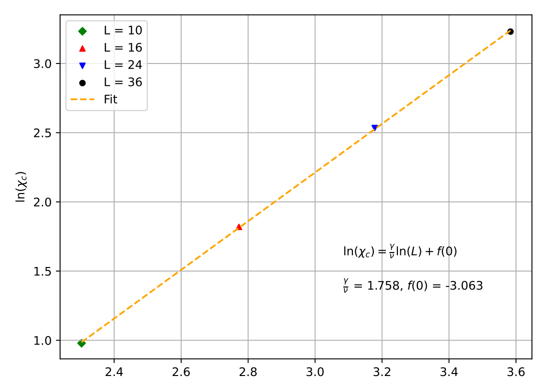

FIG. 4: The log of the maximum susceptibility, $\chi(T_c(L))$, versus $\ln(L)$. A linear fit is shown for γ/ν.

The magnetization M as a function of T is shown in Fig. 6, where we observe the finite-size scaling effect due

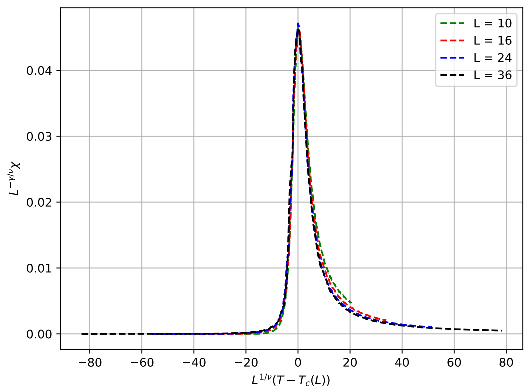

FIG. 5: $L^{-\gamma/\nu}\chi$ as a function of the scaling variable $L^{1/\nu}(T - T_c(L))$.

to the changing slope of the distribution for each system size near the critical temperature. Similarly to the susceptibility, we plot $L^{\beta/\nu}M$, as shown in Fig. 7, where β/ν is taken to be 0.25. The curves for the different system sizes then all meet at a critical point $T_c' = 2.295$, which deviates from the accepted critical temperature by 1.14%.

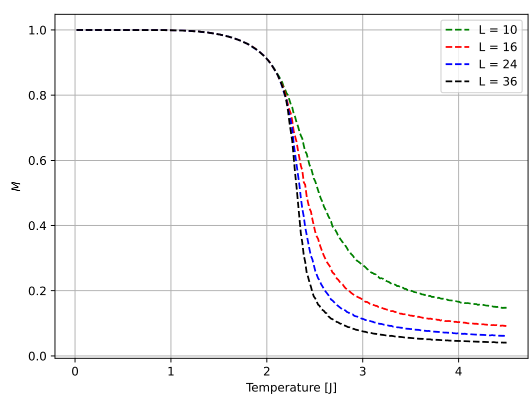

FIG. 6: Magnetization M as function of T.

We further plot $L^{\beta/\nu}M$ as a function of the scaling variable $L^{1/\nu}(T - T_c'(L)$ in Fig. 8, where T_c' is now given by the point of intersection of the curves in Fig. 7. Like in the susceptibility case shown in Fig. 5, the magnetization curves collapse onto each other near the critical region.

The specific heat C as a function of T is shown in Fig. 9, where the maxima of the specific heat, C_c, and the critical temperature in which they occur, T_c', are presented. Fig. 10 shows a plot of these critical temperatures as a function of $L^{-1/\nu}$, where $\nu = 1$. Similarly to Fig. 3, we utilize the finite-size scaling relation of Eqn. 17 and linear fit to determine the critical temperature as $L \to \infty$. Here $T_c' = 2.277$, which deviates from the exact value by 0.34%.

The α exponent of the 2D Ising model describing the divergence of the specific heat vanishes, $\alpha = 0$. This in turn implies that the specific heat diverges logarithmically. This is shown in Fig. 11, where the maximum of the heat capacity C_c is plotted as a function of $\ln(L)$. The linear behavior indicates that as L grows, C_c grows logarithmically and ultimately diverges in the $L \to \infty$

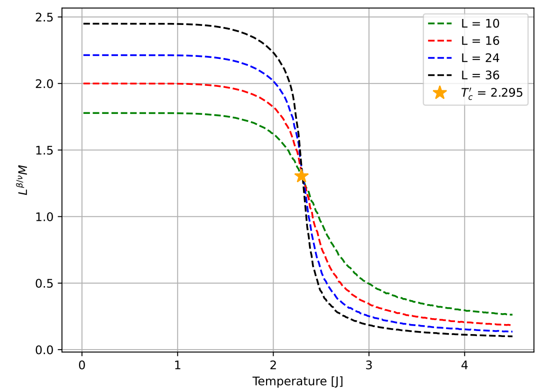

FIG. 7: $L^{\beta/\nu}M$ as a function of T. The intersection point gives T_c'.

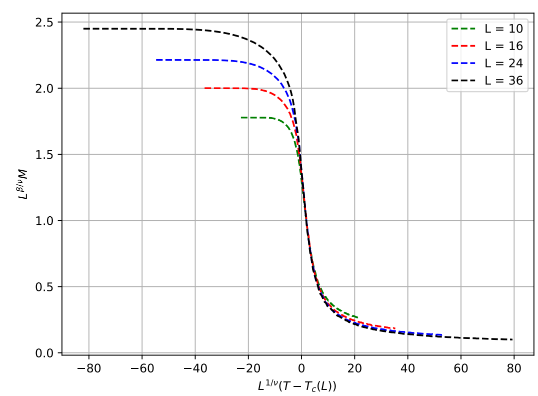

FIG. 8: $L^{\beta/\nu}M$ as a function of the scaling variable $L^{1/\nu}(T - T_c'(L)$.

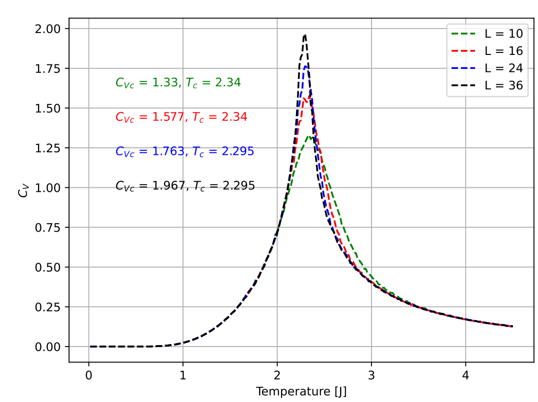

FIG. 9: Specific heat C as a function of T.

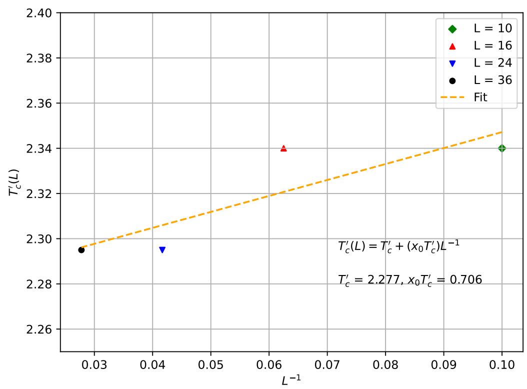

FIG. 10: $T_c'(L)$ as a function of L^{-1}, with a linear fit of Eqn. 17, where T_c is replaced with T_c', the location of the peak in the heat capacity.

limit.

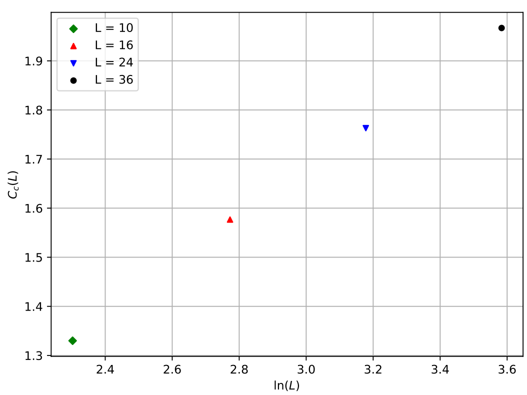

FIG. 11: $C_c(L)$ as a function of $\ln(L)$. The linear behavior indicates a logarithmic divergence in C.

The entropy per spin can be calculated from the specific heat as follows

$$S(T) = \int_0^T \mathrm{d}T' \frac{C(T')}{T'}, \tag{19}$$

where we note that $S(T \to \infty) = \ln(2)$ for the Ising model. Fig 12 shows a numerical integration of the specific heat yielding the entropy. As shown, in the large T limit, the distribution asymptotically approaches $\ln(2)$ as expected.

Using the entropy distribution, we can calculate the free energy

$$F = E - TS, \tag{20}$$

which is plotted in Fig. 13. As shown, in the high temperature limit as $S \to \ln(2)$, we see the free energy behave linearly with a slope that approaches $\ln(2)$.

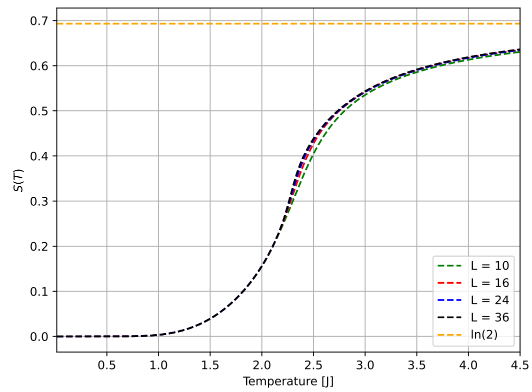

FIG. 12: Entropy S as a function T from numerically integrating $C(T)/T$. $S(T)$ asymptotically approaches $\ln(2)$.

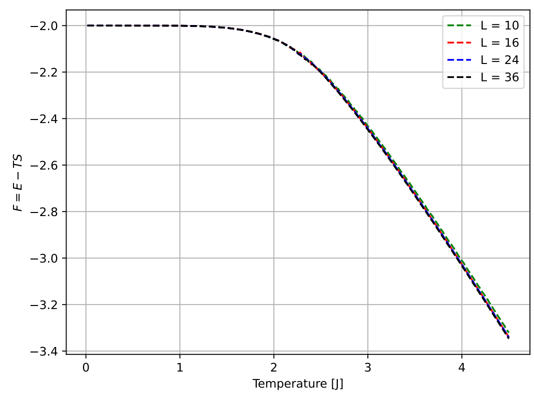

FIG. 13: Free energy $F = E - TS$ as a function of T.

IV. CONCLUSIONS

In this paper, we've presented a simulation of the 2D Ising model using the Metropolis algorithm. The simulation results, including the calculation of the critical temperature associated with a magnetic phase transition of the model are described in Sec. III. We observe $\lesssim 1\%$ deviation from the exact value of T_c by applying finite-size scaling methods.

V. ACKNOWLEDGMENTS

Thank you for the wonderful semester Hector! I found your class both enlightening and entertaining, and greatly appreciate the effort you've put into teaching this term. Hope you enjoy the holiday season!

[1] https://github.com/gabrielpmatos/ising/tree/main.
[2] M. Le Bellac, F. Mortessagne, and G. G. Batrouni, *Equilibrium and Non-Equilibrium Statistical Thermodynamics* (Cambridge University Press, 2004).

APPENDIX

For answers to the questions in Le Bellac et al., please see the discussion associated with the following:

- Q1: see Sec. II, The Metropolis Algorithm
- Q2: see Sec. III, and github.
- Q3: see Fig. 1.
- Q4: see Fig. 2 and Fig. 3.
- Q5: see Fig. 4 and Fig. 5.
- Q6: see Fig. 6, Fig. 7, and Fig. 8.
- Q7: see Fig. 9, Fig. 10, and Fig. 11.
- Q8: see Fig. 12 and Fig. 13.